Molecular Biology of the Cell
Vol. 17, 2200–2211, May 2006

# Casein Kinase II and Calcineurin Modulate TRPP Function and Ciliary Localization[D]

**Jinghua Hu,*† Young-Kyung Bae,†‡ Karla M. Knobel,*† and Maureen M. Barr*†**

*Division of Pharmaceutical Sciences, ‡Laboratory of Genetics, and †School of Pharmacy, University of Wisconsin, Madison, WI 53705

Submitted October 11, 2005; Revised February 2, 2006; Accepted February 8, 2006
Monitoring Editor: Martin Chalfie

**Cilia serve as sensory devices in a diversity of organisms and their defects contribute to many human diseases. In primary cilia of kidney cells, the transient receptor potential polycystin (TRPP) channels polycystin-1 (PC-1) and polycystin-2 (PC-2) act as a mechanosensitive channel, with defects resulting in autosomal dominant polycystic kidney disease. In sensory cilia of *Caenorhabditis elegans* male-specific neurons, the TRPPs LOV-1 and PKD-2 are required for mating behavior. The mechanisms regulating TRPP ciliary localization and function are largely unknown. We identified the regulatory subunit of the serine-threonine casein kinase II (CK2) as a binding partner of LOV-1 and human PC-1. CK2 and the calcineurin phosphatase TAX-6 modulate male mating behavior and PKD-2 ciliary localization. The phospho-defective mutant PKD-2$^{S534A}$ localizes to cilia, whereas a phospho-mimetic PKD-2$^{S534D}$ mutant is largely absent from cilia. Calcineurin is required for PKD-2 ciliary localization, but is not essential for ciliary gene expression, ciliogenesis, or localization of cilium structural components. This unanticipated function of calcineurin may be important for regulating ciliary protein localization. A dynamic phosphorylation-dephosphorylation cycle may represent a mechanism for modulating TRPP activity, cellular sensation, and ciliary protein localization.**

## INTRODUCTION

Many eukaryotic cells possess cilia (Rosenbaum and Witman, 2002). In mammals, sensory or primary cilia can sense a wide range of environmental stimuli, including light (by photoreceptors), odorants (by olfactory cilia), and urine flow (by primary kidney cilia). All sensory (or primary) cilia share a similar internal structure consisting of a "9 + 0" axoneme that contains nine double microtubules but not the central pair of doublets found in motile cilia. Membrane-bound receptors and signaling molecules are enriched within the cilium. Defects in cilia formation or function have been implicated in many human diseases, including autosomal dominant polycystic kidney disease (ADPKD; Rosenbaum and Witman, 2002).

ADPKD affects 1 in 1000 individuals and is caused by defects in polycystin-1 (PC-1, encoded by *PKD1*) or polycystin-2 (PC-2, encoded by *PKD2*; reviewed in Igarashi and Somlo, 2002). PC-1 is a 4302 amino acid protein with a large extracellular domain, a G protein–coupled receptor proteolytic site (GPS), 11 transmembrane (TM) domains, and an intracellular C-terminus (Hughes *et al.*, 1995). The polycystin/lipoxygenase/alpha-toxin (PLAT) domain is located in the first cytoplasmic loop between TM1 and TM2 and has been postulated to be involved in membrane–protein or protein–protein interactions (Bateman and Sandford, 1999). The PLAT domain is conserved in all PC-1 family members and also found in a variety of membrane or lipid associated proteins. PC-1 and PC-2 are members of the transient receptor protein polycystin (TRPP) family of TRP channels (Mochizuki *et al.*, 1996) and act as a nonselective cation channel (reviewed in Igarashi and Somlo, 2002; Delmas, 2004). TRP channels have been implicated in a plethora of sensory modalities (Clapham, 2003). PC-2 forms a mechano-sensitive channel with PC-1 and localizes in kidney cilia (Nauli *et al.*, 2003). Although our understanding of the functional role and subcellular location of the polycystins has increased, little is known about the mechanisms that dynamically regulate this important ciliary sensory complex.

Many of the human cystic kidney disease genes required for ciliogenesis or sensation have counterparts in the nematode *Caenorhabditis elegans* (Barr, 2005). A simple approach to understanding cilia development, morphogenesis, and sensory function is to use the genetics, simple nervous system, and transparent anatomy of *C. elegans*. These features enable the study of TRPP function and subcellular localization in an intact, living animal. LOV-1 and PKD-2 are the *C. elegans* homologues of PC-1 and PC-2, respectively (Barr and Sternberg, 1999; Barr *et al.*, 2001). *lov-1* and *pkd-2* mutants are specifically defective in the male mating sensory behaviors of response (Rsp) and location of vulva (Lov). *lov-1* and *pkd-2* are expressed in the 21 male-specific ciliated sensory neurons that mediate response (ray RnBs), vulva location (hook HOB), and possibly chemotaxis to mates (head CEMs; see Figure 1a). These male sensory neurons have one common structural feature: all have long dendrites that end in exposed ciliated sensory endings. LOV-1 and PKD-2 are concentrated in the sensory cilia of these neurons. The fact that the PC-1 PLAT domain, TRPP sensory function, and TRPP ciliary localization are evolutionarily conserved makes *C. elegans* an excellent model system for studying the polycystins, the molecular mechanisms underlying ADPKD, and ciliary protein localization and function (Barr and Sternberg, 1999; Barr *et al.*, 2001; Hu and Barr, 2005; Peden and Barr, 2005).

This article was published online ahead of print in *MBC in Press* (http://www.molbiolcell.org/cgi/doi/10.1091/mbc.E05–10–0935) on February 15, 2006.

[D] The online version of this article contains supplemental material at *MBC Online* (http://www.molbiolcell.org).

Address correspondence to: Maureen M. Barr (mmbarr@pharmacy.wisc.edu).

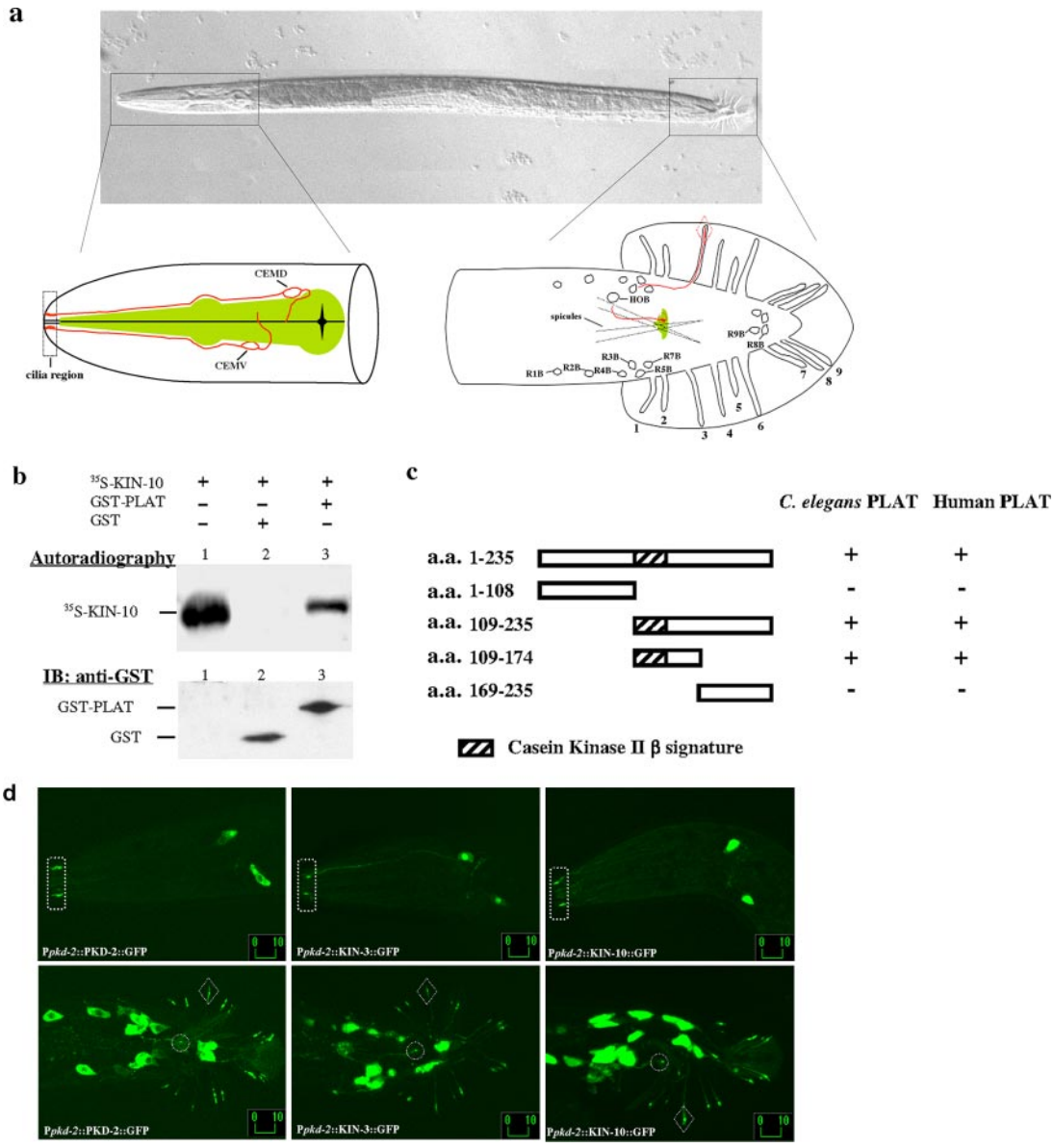


**Figure 1.** CK2 interacts with the LOV-1 and PC-1 PLAT domain and enriches in the cilia of male specific neurons. (a) Anatomy of *C. elegans* male and PKD-2–expressing neurons. Top, DIC side view image of an adult *C. elegans* male oriented head (left) to ventral up tail (right). Bottom, *lov-1* and *pkd-2* are expressed in male head CEM neurons (left) and tail ray RnB and hook HOB neurons (right). The cilium, dendrite, cell body, and axon of the CEMD (dorsal CEM) and CEMV (ventral CEM) neuron are drawn in the male head diagram. CEMD and CEMV are arranged as left-right pairs (one side shown here). Cilia are in the nose region (dashed rectangular box). The pharynx is green. Positions of nuclei of all *lov-1* and *pkd-2* expressing cells in the *C. elegans* adult male tail, modified from (Sulston *et al.*, 1980). Ray neurons are arranged as left-right bilateral pairs (ventral up view shown here). The male tail has nine bilaterally arranged rays (numbered 1–9, anterior to posterior) required for response and turning behaviors (Liu and Sternberg, 1995). HOB is an asymmetric ciliated hook neuron that mediates vulva location behavior (Liu and Sternberg, 1995). For simplicity, only the dendrite of R3B left and HOB is shown. The R3B cilium is indicated by a dashed rectangular box. (b) A GST pulldown assay demonstrates a direct in vitro interaction between KIN-10 and the LOV-1 PLAT domain. In vitro–translated $^{35}$S-labeled KIN-10 protein was incubated with GST or GST-PLAT (amino acids 2112–2302). Autoradiography shows $^{35}$S-labeled KIN-10 protein is specifically retained in the GST-PLAT column. A Western blot developed with an anti-GST antibody detects GST and GST-PLAT. (c) Y2H mapping reveals the CK2$\beta$ signature domain of KIN-10 mediates interaction with the PLAT domains of human PC-1 and *C. elegans* LOV-1. Different *kin-10* fragments were cloned into the Y2H AD vector pGADT7. The *C. elegans* and human PLAT domain (amino acids 3164–3349) were engineered into the Y2H BD vector pGBKT7. Y2H interactions were accessed by growth ability on SD-Leu-Trp-His-Ade plates. (d) Confocal micrographs of P*pkd-2*::PKD-2::GFP, P*pkd-2*::KIN-3::GFP (using *pkd-2* promoter to drive KIN-3::GFP fusion protein expression) and P*pkd-2*::KIN-10::GFP (using *pkd-2* promoter to drive KIN-10::GFP fusion protein expression) transgenic males. PKD-2 localizes to cilia and cell bodies (excluding nuclei) of male-specific neurons. KIN-3 and KIN-10 are localized and enriched in the cilia of the male-specific RnB, HOB and CEM neurons. KIN-3 and KIN-10 also localize weakly in dendrites and axons and strongly in cell bodies (especially in nuclei). Dashed rectangular boxes show the ciliary zone of the CEM neurons. Dashed circles show the ciliary zone of HOB neuron. Dashed diamond boxes show the ciliary zone of RnB neuron in ray 3. Labeled bars indicate length in micrometer ($\mu$m).

Protein phosphorylation by the coordinated activities of protein kinases and phosphatases is central to many signal transduction pathways. Here we show that casein kinase II and calcineurin/protein phosphatase 2B (PP2B) modulate PKD-2 function and ciliary localization. We find that the regulatory subunit of casein kinase II (CK2$\beta$/KIN-10) interacts with the PLAT domain of both human PC-1 and *C. elegans* LOV-1. We demonstrate that CK2 and the $Ca^{2+}$-activated phosphatase calcineurin act antagonistically to regulate PKD-2. We use a set of genetic and molecular manipulations to ask whether phosphorylation state affects polycystin function and ciliary localization in vivo. We find that a "phospho-defective" PKD-2 mutant protein trafficks normally to cilia but exhibits attenuated function, whereas a "phospho-mimetic" PKD-2 is defective in both function and ciliary localization. We show that *tax-6* regulates PKD-2 ciliary localization but not ciliogenesis or gene expression. We propose that a dynamic phosphorylation cycle modulates normal polycystin function and ciliary distribution.

## MATERIALS AND METHODS

### *Strains and Alleles*

Nematode culturing and genetics were performed by standard techniques (Brenner, 1974). *him-5(e1490)* (LGV) was used as the wild-type (Hodgkin, 1983). The following mutations were used: LGI, *kin-10(tm1283)*, *kin-3(gk389)*; LGII, *rrf-3(pk1426)*, *lov-1(sy582)*; LGIII, *pha-1(e2123ts)*; LGIV, *pkd-2(sy606)*, *tax-6(p675)*, and *tax-6(jh107)*; and LGV, *myIs4(PKD-2::GFP + ccGFP)*.

Our molecular analysis of the *kin-3(gk389)* deletion allele indicates that the VC928 genetic background is complex. The VC928 strain is homozygous for the *gk346* deletion, but PCR results show that it also contains a wild-type *kin-3* copy on the chromosome. This wild-type copy could function to balance *VC928* strain from lethal effects caused by *gk346* allele, resulting in viable animals. Based on CK2 function in many essential processes, the lethal phenotype of the *kin-10(tm1283)* allele, and the *kin-3* RNAi phenotypes of Emb(ryonic lethality) and Ste(rility), a null allele of *kin-3* should be inviable. To support this prediction, a new *kin-3* deletion allele, *ok1516*, is recently available. Unlike *gk389*, the *kin-3(ok1516)* deletion is homozygous lethal according to the Vancouver Gene Knockout Laboratory: http://aceserver.biotech.ubc.ca/cgi-bin/stable/strain.pl?class=Strain;name=VC1096.

### *Molecular Biology Techniques*

Details of plasmid constructions are available upon request. Standard procedures were used for recombinant DNA manipulations.

### *Transgenic Animals*

We constructed transgenic lines by injecting plasmid DNA (100–200 ng/ul) using standard protocols (Mello and Fire, 1995). In all experiments the plasmid pBX containing the wild-type *pha-1(+)* gene was used as a cotransformation marker in the *pha-1(ts)* strain (Granato *et al.*, 1994).

### *Yeast Two-Hybrid Screen*

The yeast strain AH 109 (Clontech, Palo Alto, CA) was used for yeast two-hybrid (Y2H) experiments. Bait proteins were expressed in the GAL4 DNA-binding domain (DNA-BD) vector, pGBKT7. A cDNA library derived from mix-staged *him-5* animals was constructed in the GAL4 activation domain (DNA-AD) vector, pGAD GH (Hu and Barr, 2005). The PLAT domain of *C. elegans* LOV-1 (amino acids: 2112–2302) and human PC-1 (amino acids: 3164–3349) were used as baits in Y2H hybrid assays. Protein–protein interactions were accessed by growth rate on SD-Leu-Trp-His-Ade high-stringency plates and $\beta$-galactosidase filter assays. KIN-10 did not interact with the cytoplasmic carboxy termini of worm LOV-1, human PC-1, worm PKD-2, or human PC-2 and various other controls (unpublished data), demonstrating specificity of the KIN-10 and PLAT domain interaction.

### *In Vitro Binding*

In vitro–translated Y2H candidate KIN-10 protein was produced with the TNT-quick coupled transcription/translation system (Promega, Madison, WI) by using [$^{35}$S]methionine (Amersham Pharmacia Biotech, Piscataway, NJ). A GST-fused LOV-1 PLAT domain was produced in the bacteria strain BL21(DE3) and incubated with in vitro–translated KIN-10 in 500 $\mu$l binding buffer (20 mM Tris-HCl, pH 7.5, 150 mM NaCl, 5 mM $MgCl_2$, 2 mM DTT, 0.05% NP40) at 4°C for 30 min. Glutathione-Sepharose 4B, 25 $\mu$l, was added to the reaction and incubated at 4°C for an additional 2 h or overnight. After three washes with binding buffer, bound proteins were resuspended in 50 $\mu$l 1× Laemmli buffer and then 10-$\mu$l samples were boiled and separated by 10% SDS-PAGE. Proteins were visualized by Coomassie staining. The dried gel was exposed for autoradiography. [$^{35}$S]-KIN-10 binds to GST-PLAT but not GST alone, indicating that KIN-10 binds directly to the PLAT domain of LOV-1 (Figure 1b).

### *Imaging Analysis and Fluorescence Quantitation*

Epifluorescence microscopy experiments were carried out by using a Zeiss Axioplan2 Imaging system (Thornwood, NY) and photographed with an Orca-ER camera. Confocal experiments were carried out on a Bio-Rad MRC-1024 laser scanning confocal microscope (Richmond, CA). To quantitate cilium/cell body fluorescence intensity ratio, L4 animals were picked and cultured at 16°C for 20–24 h. Confocal or epifluorescence images were taken of adults. Overexposure was avoided by ensuring fluorescence was not saturated in any areas of the images. Mean fluorescence intensities of the cilium (including the axoneme and transition zone), the corresponding cell body (including the nucleus), and background (area without the animal) were quantified using OpenLab software (Improvision, Lexington, MA). Cilium/cell body fluorescence intensity ratios were calculated using the following formula: (mean cilium fluorescence intensity − background fluorescence intensity)/(mean cell body fluorescence intensity − background fluorescence intensity).

### *RNA Interference and Mating Behavior Assays*

Multiple RNA interference (RNAi) methods were used. For heat shock–inducible RNAi mediated by the inverted-repeat (IR) genes (HS-IR-RNAi), we constructed IR genes as described (Tavernarakis *et al.*, 2000; Wang and Barr, 2005). Transgenic lines carrying IR plasmids were generated. Mix-staged transgenic animals were heat shocked for 4 h at 35°C, before returning to 15°C. After 63–67 h at 15°C, L4 males were transferred to new plates for culturing another 14 h at 15°C. Mating behaviors were scored as described (Barr and Sternberg, 1999). For tissue-specific RNAi (TS-IR-RNAi), we constructed IRs whose transcription is under the control of the *pkd-2* promoter. Transgenic lines were generated, and males were scored for mating behaviors. For feeding RNAi, RNAi bacteria clones were obtained from MRC Geneservice (Cambridge, UK). The *kin-3* RNAi feeding clone was generated by inserting the 600-base pair *kin-3* cDNA into the NcoI site of the plasmid L4440, followed by transformation into the *Escherichia coli* HT115(DE3) strain. Double-stranded RNA (dsRNA) producing bacteria were grown in LB with 50 ng/ml ampicillin overnight at 37°C and seeded onto NGM agar plates including additives (1 mM IPTG, 50 ng/ml ampicillin). The following day, 6–8 L4 stage RNAi sensitive *rrf-3; him-5* hermaphrodites (Simmer *et al.*, 2002) were transferred onto feeding plates and incubated ~72 h at 15°C. L4 males (n = 20–50) were picked to new feeding plates seeded with feeding RNAi bacteria and cultured 14 h at 15°C, and the mating behaviors of adult males were scored. In all experiments, at least 24 animals were scored per experimental trial. Triplicate trials were performed for each line to obtain statistical data. All behavioral assays were done with the experimenter completely blinded to the sample.

### *Immunoprecipitation*

HA-tagged PKD-2 or HA-tagged PKD-2$^{S534A}$ expressing HEK 293T cells were lysed in buffer supplemented with protease and phosphatase inhibitors (50 mM Tris-HCl, pH 8.0, 1% NP-40, 150 mM NaCl, 1 mM phenylmethylsulfonyl fluoride, 1 $\mu$g/ml pepstatin, 1 $\mu$g/ml aprotinin, 1 $\mu$g/ml leupeptin, 1 $\mu$g/ml $Na_3PO_4$, 1 mM EDTA). For immunoprecipitation, whole cell lysates were precleared with protein A-agarose beads (Amersham Pharmacia Biotech). A mouse anti-HA IgG1 (HA.11, clone 16B12, Covance, Madison, WI) was added to precleared whole cell lysates and incubated overnight at 4°C. Protein-A-agarose beads, 30 $\mu$l, were added to each of the incubations for 4 h at 4°C. Control immunoprecipitation with mouse IgG or beads alone was also performed. The immunoprecipitated complexes were washed three times in phosphate-buffered saline, and Western blotting was performed.

### *In Vitro Kinase and Phosphatase Assays*

After immunoprecipitation, HA-PKD-2, HA-PKD-2$^{S709A}$, or HA-PKD-2$^{S534A}$ was incubated in CK2 buffer (20 mM Tris-HCl, pH 7.5, 50 mM KCl, 10 mM $MgCl_2$, 200 $\mu$M ATP, 100 $\mu$M $Na_3VO_4$) with 100 $\mu$Ci/$\mu$M [$\gamma$-$^{32}$P]ATP (Amersham Pharmacia, 3000 Ci/mM) and 500 U recombinant CK2 (NEB BioLabs, Beverly, MA; P6010S) for 30 min at 30°C. Control kinase reaction without immunoprecipitation complex was also done. The kinase assays were stopped by adding 2× Laemmli sample loading buffer and boiled for 5 min. For phosphatase assays, the HA-PKD-2 HA-PKD-2$^{S709A}$–, or HA-PKD-2$^{S534A}$–conjugated protein A beads were washed three times with phosphatase buffer (50 mM Tris-HCl, pH 7.0, 0.1 mM $CaCl_2$) after the CK2 kinase reaction. The beads were incubated in the phosphatase assay system (50 mM Tris-HCl, pH 7.0, 0.1 mM $CaCl_2$, 1 mM $NiCl_2$, 125 $\mu$g/ml BSA, 10 $\mu$g/ml calmodulin) with 1 U/ml calcineurin/PP2B (Upstate, Cat. 14-446) for 30 min at 37°C. The reactions were stopped by adding 2× Laemmli sample loading buffer and boiled for 5 min. The samples were then centrifuged and loaded onto a 10% SDS-polyacrylamide gel. After electrophoresis, the gel was dried and autoradiography was performed. Western blotting with anti-HA antibody was performed to quantitate protein levels.

## RESULTS

### *The CK2 β Regulatory Subunit Interacts with C. elegans LOV-1 and Human PC-1*

The PLAT domain is a highly conserved structure in all PC-1 family members, yet its function remains unknown. We reported previously that overexpression of the PLAT domain of the *C. elegans* PC-1 homolog, LOV-1, dominantly interferes with *C. elegans* male sensory behaviors but is insufficient for ciliary localization (Hu and Barr, 2005). We sought to determine the functional role of the PLAT domain by identifying binding partners via a yeast two-hybrid screen (Hu and Barr, 2005). We find that KIN-10, the regulatory β subunit of casein kinase II (CK2), interacts with the PLAT domain of LOV-1 in a yeast two-hybrid assay (Figure 1c) and GST pulldown assay (Figure 1b). KIN-10 also interacts with the PLAT domain of human PC-1 (Figure 1c) but not the carboxy cytoplasmic tails of LOV-1 or PKD-2 (unpublished data).

Protein kinase CK2 is a ubiquitous serine/threonine kinase comprised of two catalytic α and two regulatory β subunits (Meggio and Pinna, 2003). The CK2β subunit determines kinase substrate specificity (Pinna, 2002; Litchfield, 2003). *C. elegans* CK2 α catalytic and β regulatory subunits are encoded by *kin-3* and *kin-10*, respectively (http://www.wormbase.org). We mapped the region of KIN-10 region responsible for the interaction with the PLAT domain of both human PC-1 and *C. elegans* LOV-1. The C-terminus of KIN-10 (amino acids 109–174), which contains a conserved CK2 β signature domain, is the minimal PLAT binding region (Figure 1c). Based on the crystal structures of CK2 holoenzyme and the CK2β dimer, the CK2 β signature domain has been proposed to mediate β subunit dimerization and form a protein–protein interaction site (Chantalat *et al.*, 1999; Niefind *et al.*, 2001).

### *CK2 Is Present in Cilia*

A prerequisite for a physiologically relevant interaction between CK2 and the polycystins is coexpression and localization in the same subcellular compartment. *kin-3/CK2α* and *kin-10/CK2β* are widely expressed throughout development in both males and hermaphrodites, predominantly in many head neurons and the intestine. *kin-3* and *kin-10* are coexpressed with *lov-1* and *pkd-2* in the male-specific CEM head neurons and ray RnB and hook HOB tail neurons (Supplementary Figure 1). We next examined the subcellular localization of CK2 using the 1.3-kb *pkd-2* promoter to restrict expression of KIN-3::GFP and KIN-10::GFP (P*pkd-2*::KIN-3::GFP and P*pkd-2*::KIN-10::GFP) to only the polycystin-expressing cells. In *pkd-2*–expressing cells, KIN-3::GFP and KIN-10::GFP are enriched in cilia and also found in cell bodies (including nuclei), dendrites, and axons (Figure 1d). Although CK2 has been found in nearly every compartment of the eukaryotic cell (reviewed in Faust and Montenarh, 2000), this is the first description of CK2 enrichment within a primary cilium, a restricted subcellular compartment dedicated to sensory functions.

### *CK2 Modulates TRPP-dependent Male Sensory Behaviors*

The role of CK2 in polycystin-mediated response and vulva location behaviors was examined. *kin-10* and *kin-3* null mutants are homozygous lethal, precluding adult behavioral analysis (refer to *Materials and Methods* for strain information). To study the function of CK2 in *C. elegans* male mating behavior, *kin-3* and *kin-10* were knocked down by using multiple RNAi methods (Hu and Barr, 2005; Wang and Barr, 2005). Feeding RNAi directed to either *kin-3* or *kin-10* produced similar phenotypes: Emb (embryonic lethality), Gro (Slow growth), and pVul (protruding vulva; unpublished data; Fraser *et al.*, 2000). For those males that survived to adulthood, *kin-3* and *kin-10* feeding RNAi caused Rsp but not Lov mating behavior defects (Figure 2a). IR plasmids producing dsRNA are effective at knocking down gene function in neurons and are particularly valuable for temporal or tissue-specific gene knockdown using appropriate promoters (Tavernarakis *et al.*, 2000). Either the heat shock promoter (HS-IR-RNAi for heat shock–inducible inverted repeat RNAi) or *pkd-2* promoter (TS-IR-RNAi, for tissue-specific expressed inverted repeat RNAi) was used to drive expression of *kin-10* or *kin-3* cDNA IRs. Knockdown of *kin-10* or *kin-3* function by either HS-IR-RNAi or TS-IR-RNAi consistently resulted in both Rsp and Lov defects (Figure 2, b and c). Negative controls to unrelated genes do not affect male mating behaviors (unpublished data). These results indicate that CK2 functions in a cell autonomous manner to modulating response and vulva location behavior.

HS-IR *kin-3* RNAi was more potent in reducing response than TS-IR *kin-3* RNAi (compare Figure 2, b and c). The heat shock promoter is expressed broadly, suggesting that KIN-3/CK2α may function in both polycystin-expressing and polycystin-nonexpressing cells to modulate response behavior. These data also indicate that there are cells in addition to the polycystin-sensory neurons (CEMs, RnBs, and HOB) that control the response step of mating behavior.

Laser ablation of the neurons expressing *lov-1* and *pkd-2* causes more severe behavioral defects than mutations in *lov-1* and *pkd-2* (for example, 0% vulva location efficiency for HOB ablated animals vs. ~25% vulva location efficiency for *lov-1* and *pkd-2* mutants; Liu and Sternberg, 1995; Barr and Sternberg, 1999; Barr *et al.*, 2001). If CK2 and the polycystins act in different pathways or if knocking down CK2 expression causes general developmental defects of the targeted sensory neurons, we would observe an additive effect with more severe Rsp and Lov defects than loss of either alone. To determine if CK2 and the polycystins function in the same or a parallel genetic pathway, the effects of *kin-3* and *kin-10* RNAi were examined in *lov-1* and *pkd-2* null mutant backgrounds. The behavioral defects of *lov-1* and *pkd-2* mutants are not exacerbated by *kin-3* or *kin-10* TS-IR RNAi (Figure 2, d and e). These results indicate that CK2, *lov-1*, and *pkd-2* act in the same genetic pathway regulating mating behavior and that the interaction between KIN-10 and LOV-1 is physiologically relevant.

To determine if LOV-1 or PKD-2 are required for CK2 localization, we quantified the ciliary expression levels of KIN-3::GFP and KIN-10::GFP in wild-type and *lov-1* or *pkd-2* mutants. The levels of P*pkd-2*::KIN-3::GFP and P*pkd-2*::KIN-10::GFP in cilia is similar in wild-type and *lov-1* or *pkd-2* mutant males (unpublished data). Therefore, *lov-1* and *pkd-2* are not required for CK2 localization in cilia. To determine if CK2 is required for PKD-2::GFP localization, we quantified the ciliary expression levels in wild-type and CK2 RNAi-treated males. PKD-2::GFP localization in wild-type and *kin-3* or *kin-10* TS-IR RNAi-treated animals is comparable (unpublished data), indicating that CK2 modulates PKD-2 function but is not essential for PKD-2 ciliary localization.

### *Serine 534 Is an Important Residue for PKD-2 Function and Ciliary Localization*

The basic cellular function of CK2 is to phosphorylate and regulate substrates. There are multiple predicted CK2 phosphorylation sites in LOV-1 and PKD-2. We focused on PKD-2 for two reasons: First, CK2 has been demonstrated to phosphorylate and regulate human PC-2 (Cai *et al.*, 2004; Kottgen *et al.*, 2005). Second, the LOV-1 protein is 3125 amino acids and PKD-2 is only 716 amino acids (K. M. Knobel and M. M. Barr, unpublished results), making the latter more easily manipu-

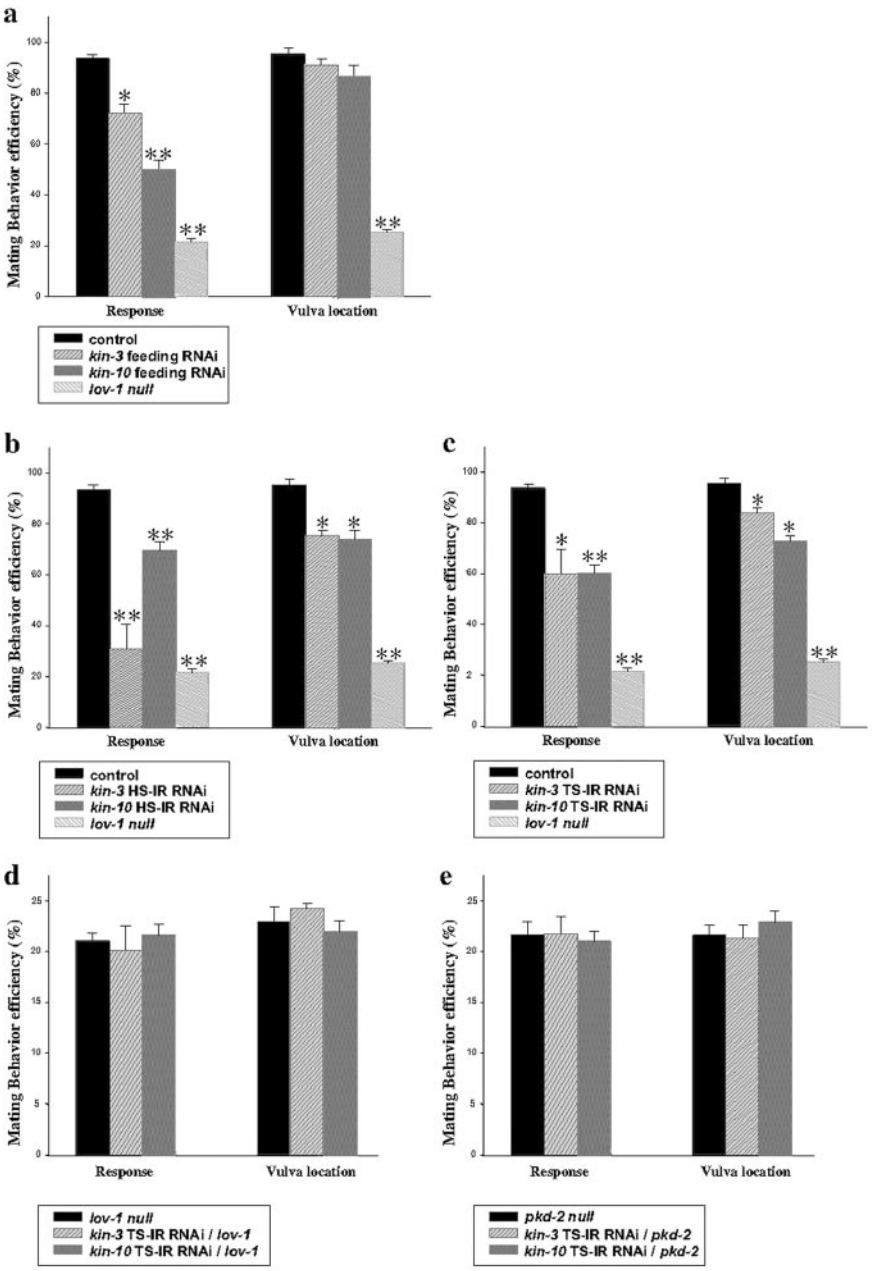


**Figure 2.** CK2 modulates male sensory behaviors and acts with *lov-1* and *pkd-2* in same genetic pathway. (a–c) Knocking down *kin-3* and *kin-10* in wild-type *C. elegans* by various RNAi methods disrupts male mating behaviors. (a) Feeding RNAi was performed on RNAi sensitive strain *rrf-3(pk1426); him-5*. A bacterial strain of the *kin-10* feeding RNAi clone (I-4G07) was obtained from MRC Geneservice, the *kin-3* feeding RNAi clone was generated in our lab (*Materials and Methods*). After feeding RNAi, response but not vulva location defects were observed. (b) HS-IR RNAi, heat shock–induced inverted-repeat RNAi, inverted-repeat *kin-3* and *kin-10* cDNA and (c) TS-IR RNAi, tissue specific promoter driving IRs of *kin-3* and *kin-10* cDNAs produced significant defects in both response and vulva location behaviors. (d and e) Knocking down *kin-3* or *kin-10* in a *lov-1* or *pkd-2* null mutant does not further exacerbate the mating behavior defects, suggesting that *kin-3* and *kin-10* function in same genetic pathway with *lov-1* and *pkd-2*. Note that the *Y*-axis scales in a–c and d and e are different. In this and all subsequent behavioral analyses, at least 24 animals were scored per trial. For each line, experiment trials were done in triplicate trials to obtain statistical data. Figures were generated using Sigmaplot5 (Jandel Scientific, San Rafael, CA). Data are represented as mean ± SEM. * $p < 0.05$ compared with control; ** $p < 0.01$ compared with control.

lated. GFP-tagged wild-type PKD-2 rescues *pkd-2* null mutant mating behavior defects and localizes to cilia, similar to endogenous PKD-2 (Barr *et al.*, 2001; Bae, Y. K., Qin, H., Knobel, K. M., Hu, J., Rosenbaum, J. L., and Barr, M. M., unpublished results). Therefore, male mating behavior and ciliary localization are powerful readouts of polycystin function (Barr and Sternberg, 1999; Barr *et al.*, 2001; Peden and Barr, 2005). The cytoplasmic regions of PKD-2 contain 7 predicted CK2 sites: 2 in the N-terminus ($S^{58}$, $S^{73}$) and 5 in the C-terminus ($S^{534}$, $T^{577}$, $S^{606}$, $S^{656}$, $S^{709}$; Figure 3a). We generated "phospho-defective" PKD-2 mutants by changing individual serine or threonine sites to alanine (Greif *et al.*, 2004). Individual GFP-tagged mutagenized clones were analyzed for ability to complement *pkd-2* mutant mating behavior defects and to localize to cilia. For the latter, we measured the levels of different GFP-tagged proteins by quantitative fluorescence, comparing the relative levels of PKD-2::GFP in the cilium versus cell body and obtaining a fluorescence intensity ratio (see *Materials and Methods*). In this manner, we can also measure overall expression levels for each transgene by comparing fluorescence intensity values for cell bodies and cilia.

Only PKD-$2^{S534A}$ fails to fully rescue *pkd-2* defects (Figure 3b), suggesting that S534 is an important functional residue. The expression level and ciliary localization of GFP-tagged PKD-$2^{S534A}$ is comparable to wild-type PKD-2::GFP in male-specific neurons (compare Figures 1d and 3c). Alignment of *C. elegans* PKD-2 with *C. briggsae*, sea urchin, zebrafish, mouse, rat, and human PC-2- and PC-2-like proteins reveals that S534 is the only conserved predicted CK2 phosphorylation site (S681 in mouse PC-2 and T683 in human PC-2; Figure 3a). Evolutionary conservation of the S534 CK2 site suggests selective pressure and an important cellular function. Interestingly, *Dro-*

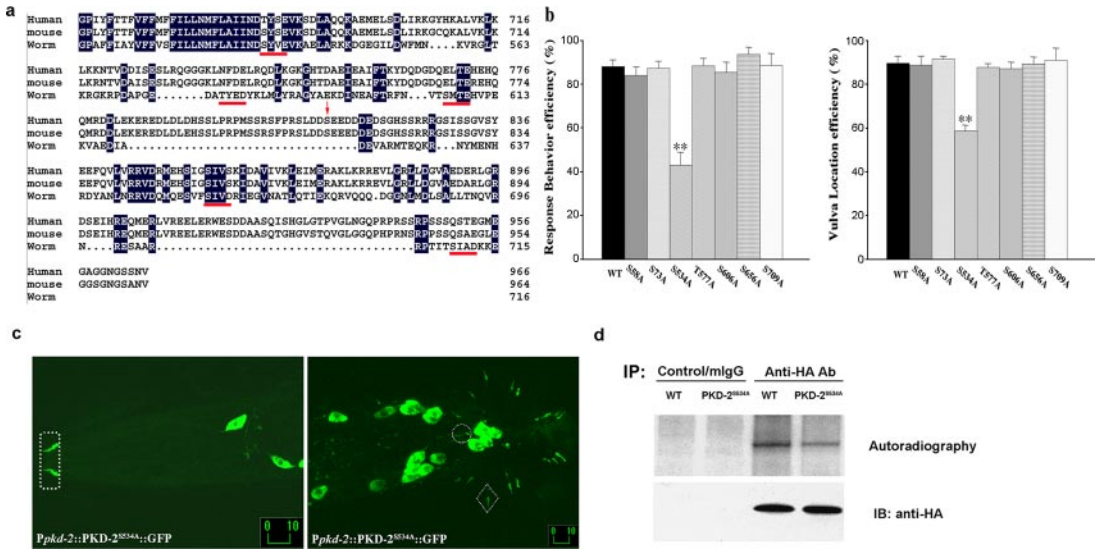


**Figure 3.** PKD-2$^{S534}$ is an important site. (a) Multiple amino acid alignment of human, mouse, and *C. elegans* polycystin-2 C-termini. Red bars indicate the five predicted *C. elegans* PKD-2 CK2 phosphorylation sites: S534, T577, S606, S656, and S709. Only the predicted S534 CK2 phosphorylation site is conserved among human, mouse, and *C. elegans*. (b) Different CK2 phosphodeficient variants of *C. elegans* PKD-2 were generated by site-mutagenesis of Serine (S) or Threonine (T) to Alanine (A), injected into *pkd-2* null animals, and the behavior of transgenic lines scored for rescue. Only S534A does not fully rescue *pkd-2* mutant defects. In all experiments, at least 24 animals were scored per trial. For each line, experiment trials were done in triplicate trials to obtain statistical data. Figures were generated using Sigmaplot5 (Jandel Scientific). Data are represented as mean ± SEM. ** $p < 0.01$ compared with control. (c) In these confocal images, PKD-2$^{S534A}$::GFP exhibits normal localization in cilia and cell bodies of male-specific neurons (compare to wild-type PKD-2::GFP in Figure 1d). Dashed rectangular boxes show the ciliary zone of the CEM neurons. Dashed circles show the ciliary zone of HOB neuron. Dashed diamond boxes show the ciliary zone of RnB neuron in ray 3. Numbers indicate the corresponding rays. Labeled bars indicate length in micrometers ($\mu$m). (d) S534 is one of CK2 phosphorylation sites on PKD-2. HA-tagged PKD-2 or HA tagged PKD-2$^{S534A}$ were transfected and expressed in HEK 293 cells. Immunoprecipitated HA-PKD-2 or HA-PKD-2$^{S534A}$ was incubated with human recombinant CK2 kinase and [$\gamma$-$^{32}$P]ATP at 30°C for 30 min, followed by electrophoresis and autoradiography. A Western blot with an anti-HA antibody was used to quantify protein concentration in each lane. With equal amounts of wild-type or S534A mutant PKD-2 protein, phosphorylation of PKD-2$^{S534A}$ is significantly lower than wild-type PKD-2.

*sophila* PKD2 does not possess this site and does not function in sensory cilia (Gao *et al.*, 2003, 2004; Watnick *et al.*, 2003).

To further explore the function of phosphorylation, we generated the GFP-tagged phospho-mimetic PKD-2$^{S534D}$ mutant. Serine or threonine to aspartate (D) substitutions might mimic phosphorylation by introducing a negative charge (Greif *et al.*, 2004). The PKD-2$^{S534D}$ construct was expressed in *pkd-2* null animals. In all eight PKD-2$^{S534D}$::GFP transgenic lines examined, none is fully rescued (Figure 4c). Strikingly, the expression level of the GFP-tagged PKD-2$^{S534D}$ protein in the cilium is greatly reduced (Figure 4, a and b, compared with Figures 1d and 3c). Because the ciliary localization of PKD-2 is critical for function, the reduction of PKD-2$^{S534D}$ in cilia may account for the failure to fully rescue the *pkd-2* mutant. Alternatively, PKD-2$^{S534D}$ may represent a dysregulated channel.

To genetically determine whether PKD-2$^{S534}$ is a direct target of CK2, we combined RNAi of CK2 with the PKD-2$^{S534D}$ point mutant. If CK2 functions on sites in addition to PKD-2 S534, we predict more severe mating defects after CK2 RNAi treatment. We observed no additive effects on mating behavior defects with CK2 RNAi and PKD-2$^{S534D}$ (Figure 4d). This experiment indicates that PKD-2$^{S534}$ is an important site that is modulated by CK2. To biochemically demonstrate that CK2 phosphorylates PKD-2, an in vitro kinase assay was performed. HA-tagged PKD-2 was expressed in HEK293T cells, immunoprecipitated with an anti-HA antibody, and incubated with purified CK2. Less phosphorylation by CK2 was detected on HA-PKD-2$^{S534A}$ than wild-type HA-PKD-2 (Figure 3d). HA-PKD-2$^{S534A}$ is still phosphorylated, indicating that S$^{534}$ is one but not the only in vitro CK2 phosphorylation site. As a control, we also compared phosphorylation level by CK2 between HA-PKD-2 and HA-PKD-2$^{S709A}$, a phosphorylation site mutant that does not visibly affect PKD-2 function or subcellular localization. No difference in phosphorylation levels between wild-type PKD-2 and PKD-2$^{S709A}$ was observed (unpublished data). Our physiological and biochemical data corroborate, showing that S534 is an important site. Endogenous PKD-2 and our PKD-2::GFP transgenes are expressed in a small number of neurons (~5% of the somatic cells in the male), and we have been unable to detect the protein by Western analysis, prohibiting in vivo analysis of PKD-2 phosphorylation.

### *TAX-6 Calcineurin Is Required for PKD-2 Ciliary Localization*

PKD-2 phosphorylation state appears to modulate its function and ciliary localization, with S534A and S534D reflecting two extreme states. Calcineurin (CaN, protein phosphatase 2B, PP2B) is a calcium-activated serine/threonine protein phosphatase that regulates the activity of several ligand-gated channels and membrane receptors (Kuhara *et al.*, 2002; Misonou *et al.*, 2004; Mohapatra and Nau, 2005; Wu *et al.*, 2005). Human TRPP channels conduct calcium (Chen *et al.*, 1999; Hanaoka *et al.*, 2000), making calcineurin an attractive candidate phosphatase. In *C. elegans*, *tax-6* encodes the catalytic subunit of calcineurin (Bandyopadhyay *et al.*, 2002; Kuhara *et al.*, 2002) and regulates several behaviors (Kuhara *et al.*, 2002; Lee *et al.*, 2004, 2005; Gottschalk *et al.*, 2005). In the hermaphrodite, *tax-6* is expressed in ciliated sensory neurons (Kunitomo *et al.*, 2005). In the male, we observed *tax-6* expression in the CEM, HOB, and

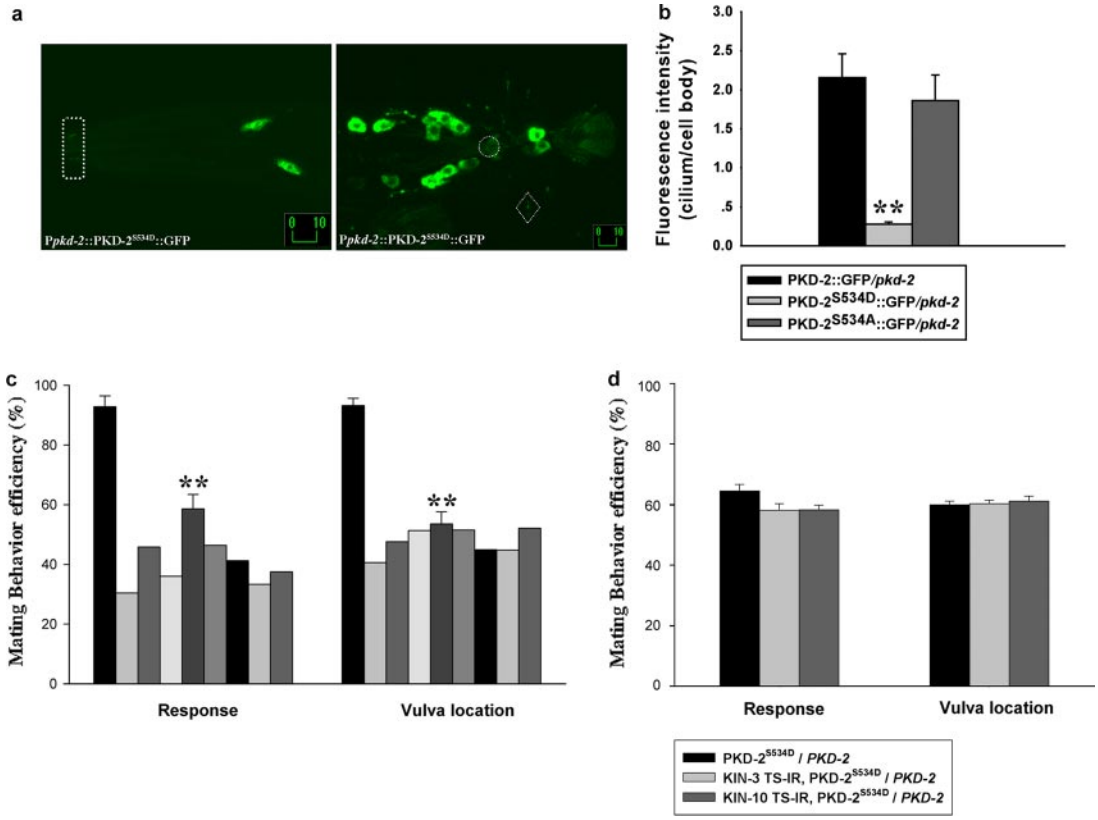


**Figure 4.** PKD-2$^{S534D}$ is not fully functional and depleted from cilia. (a) Confocal micrographs show that PKD-2$^{S534D}$::GFP is great reduced in cilia but not cell bodies. Dashed rectangular boxes show the ciliary zone of the CEM neurons. Dashed circles show the ciliary zone of HOB neuron. Dashed diamond boxes show the ciliary zone of RnB neuron in ray 3. Numbers indicate the corresponding rays. Labeled bars indicate length in micrometers ($\mu$m). (b) Quantification of the fluorescence intensity ratio of PKD-2::GFP and variants in cilium versus the corresponding cell body. PKD-2$^{S534D}$::GFP is reduced in cilia. PKD-2::GFP and PKD-2$^{S534A}$::GFP ratios are comparable. (c) PKD-2$^{S534D}$::GFP is not functional. None of the eight transgenic lines fully rescues *pkd-2* defects. For the line with most improved mating (Line 4), experiment trials were done in triplicate trials to obtain statistical data. (d) RNAi of CK2 has no further additive effect on mating behavior in the PKD-2$^{S534D}$, indicating that PKD-2$^{S534}$ is an important functional site that is phosphorylated by CK2 in vivo.

ray RnB neurons, with expression noticeably absent from ray 6, which is very similar to *lov-1* and *pkd-2* expression patterns (Figure 5a). TAX-6::GFP also localizes to cilia of these polycystin-expressing neurons (Supplementary Figure 2).

Overexpression of TAX-6::GFP results in Rsp and Lov defects, a behavioral phenotype similar to that caused by CK2 RNAi or a PKD-2$^{S534}$ phosphorylation mutation (unpublished data). Next, we examined male mating behavior and PKD-2 localization in two *tax-6* mutant backgrounds. *tax-6(p675)* is a loss-of-function allele whereas *tax-6(jh107)* is a gain-of-function allele lacking the calmodulin-binding site and autoinhibitory region (Kuhara *et al.*, 2002; Lee and Ahnn, 2004). Both loss-of-function and gain-of-function *tax-6* alleles exhibit Rsp and Lov defects (Figure 5d). However, their PKD-2 ciliary localization phenotypes are distinct. Gain-of-function *tax-6(jh107)* does not affect PKD-2 localization. Similarly, *rcn-1*, a negative regulator of calcineurin (Lee *et al.*, 2003), is also required for response and vulva location behaviors (Figure 5d) but not PKD-2::GFP ciliary localization (unpublished data). In contrast, loss-of-function *tax-6 (p675)* exhibit greatly decreased PKD-2::GFP ciliary expression (Figure 5, b and c), mirroring the PKD-2$^{S534D}$ phenotypes.

To determine whether calcineurin dephosphorylates PKD-2, an in vitro phosphatase assay was performed. As shown in Figure 5e, CK2-phosphorylated PKD-2 is dephosphorylated by calcineurin. Equivalent phosphorylation levels between PKD-2 and PKD-2$^{S534A}$ after calcineurin treatment indicate that S534 in wild-type PKD-2 is dephosphorylated by calcineurin. Residual phosphorylation indicates that not all CK2 in vitro phosphorylation sites on the PKD-2 protein are dephosphorylated by calcineurin. These data biochemically substantiate the assertion that CK2 and calcineurin function antagonistically to regulate PKD-2 phosphorylation state.

Constitutive phosphorylation of PKD-2 (by *tax-6* loss-of-function or the phospho-mimetic PKD-2$^{S534D}$) results in a loss of PKD-2 from cilia. Alternatively or perhaps additionally, *tax-6* may regulate *pkd-2* gene expression or ciliogenesis. To determine if cilia are structurally normal, we used GFP-tagged ciliary markers. Amphid and phasmid cilia were labeled with P*osm-6*::OSM-6::GFP, an intraflagellar transport (IFT) Complex B polypeptide that localizes to the ciliary base and moves along the axoneme (Collet *et al.*, 1998; Orozco *et al.*, 1999). In the *tax-6(p675)* loss-of-function mutant, cilia development, morphology, and OSM-6 motility were intact in amphid, phasmid, and male-specific sensory neurons (unpublished data). Hence, we can rule out an essential role for calcineurin in ciliogenesis. These results also indicate that *tax-6* is not required for OSM-6 expression, protein stability, ciliary localization, or motility.

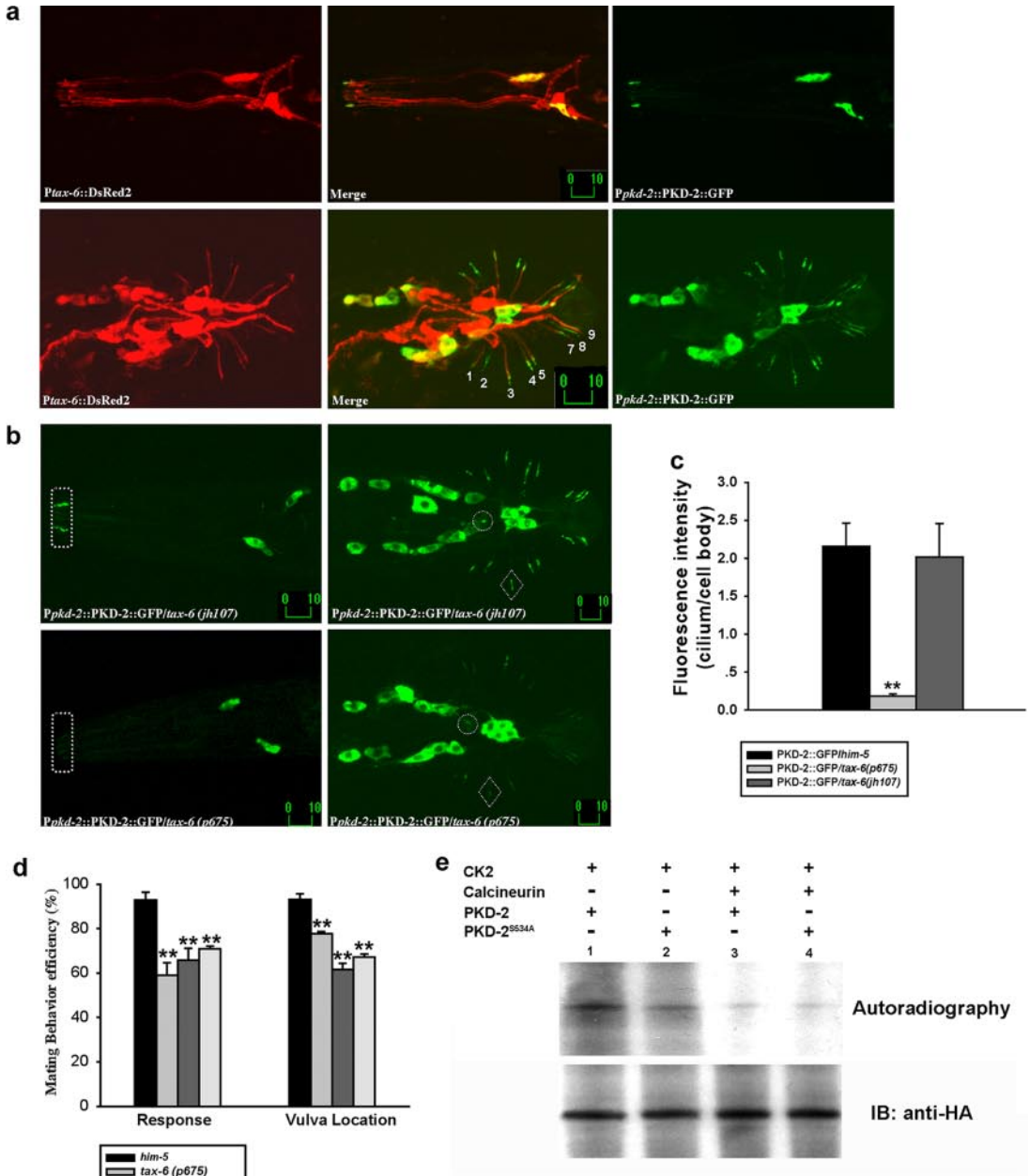


**Figure 5.** The *C. elegans* calcineurin TAX-6 is required for male sensory behaviors and PKD-2 ciliary localization. (a) Confocal micrographs of the head (top) and tail (bottom) of a transgenic male expressing P*tax-6*::DsRed2 (using *tax-6* promoter to drive DsRed2 expression) and P*pkd-2*::PKD-2::GFP. *tax-6* is coexpressed with *pkd-2*. Like *lov-1* and *pkd-2*, *tax-6* is never expressed in ray 6 (R6B). (b) Confocal micrographs and (c) quantification of PKD-2::GFP localization in *tax-6 (p675)* loss-of-function and *tax-6 (jh107)* gain-of-function mutants. PKD-2::GFP ciliary localization is normal in *tax-6 (jh107)* gain-of-function mutant, but is significantly reduced in *tax-6 (p675)* loss-of-function mutant. Dashed rectangular boxes show the ciliary zone of CEMs neuron. Dashed circles show the ciliary zone of HOB neuron. Dashed diamond boxes show the ciliary zone of RnB neuron in ray 3. Labeled bars indicate length in micrometers ($\mu$m). (c) Quantification of the fluorescence intensity ratio of PKD-2::GFP–expressing cilium to the corresponding cell body. (d) Both *tax-6 (jh107)* and *tax-6(p675)* mutant males are Rsp and Lov defective. Knocking down *rcn-1* expression in wild-type males also causes response and vulva location behaviors defects. (e) Calcineurin dephosphorylates PKD-2. Immunoprecipitated HA-PKD-2 or HA-PKD-2$^{S534A}$ was incubated with human recombinant CK2 kinase and [$\gamma$-$^{32}$P]ATP at 30°C for 30 min, washed with phosphatase buffer three times, and then incubated with calcineurin at 37°C for 1.5 h, followed by electrophoresis and autoradiography. A Western blot with an anti-HA antibody was used to quantify protein concentration to insure equivalent protein input in each level. With equal amounts of wild-type or mutant S534A PKD-2 protein, both PKD-2 and PKD-2$^{S534A}$ are dephosphorylated by calcineurin to equivalent phosphorylation levels. (f) Quantification of the fluorescence intensity ratio of PKD-2$^{S534A}$::GFP in wild-type and *tax-6(p675)* mutant.

Next, we examined the effects of the *tax-6(p675)* loss-of-function mutation on *pkd-2* expression. We found that P*pkd-2*::GFP expression is slightly higher in wild-type (~1.5-fold) than in the *tax-6(p675)* mutant (as determined by comparing cell body fluorescence intensity). Hence, calcineurin is not essential but does play a subtle role in the regulation of *pkd-2* expression. However, this result cannot explain the nearly 10-fold reduction of PKD-2 in *tax-6 (p675)* cilia (Figure 5c).

Calcineurin may affect PKD-2 ciliary localization by regulating trafficking to cilia or away from cilia. To distinguish between these models and test the hypothesis that calcium and neuronal activity are regulating PKD-2 trafficking, we took several experimental approaches. First, we examined the subcellular distribution patterns of PKD-2 in wild-type and *tax-6(p675)* late L4 larval males. Although *pkd-2* is expressed in the late L4 larval stage (just preceding adulthood), L4 males are sexually inactive (Simon and Sternberg, 2002; Lipton *et al.*, 2004). Wild-type late L4 males and wild-type adult males exhibit distinct PKD-2 ciliary localization patterns. In wild-type adult males, PKD-2 is distributed along the ciliary axoneme and accumulates in the transition zone between the cilium and dendrite (Figure 1d). In ray neurons of wild-type late L4 males, the majority of the PKD-2 protein localizes to the tip of the cilium and around the transition zone, whereas the staining along the ciliary axoneme is very weak (Figure 6a). In both wild-type and *tax-6(p675)* late L4 males, PKD-2 localization and expression levels in cilia and cell bodies are similar (Figure 6a). These data shows that PKD-2 is transcribed, translated, and localized normally in *tax-6(p675)* L4 males. In wild-type L4 males, we also observe indistinguishable PKD-2 and PKD-2$^{S534D}$ ciliary localization phenotypes, with both wild-type and the S534D phosphomimetic localizing to the ciliary tip and transition zone (Figure 6a). These results demonstrate that PKD-2$^{S534D}$ is transcribed, translated, and localized normally to cilia in L4 males. In the adult worm, decreased ciliary localization of PKD-2$^{S534D}$ or PKD-2 in *tax-6(p675)* mutant may due to the changes in a pathway that maintains PKD-2 ciliary localization or regulates PKD-2 removal from cilia.

To further examine the effects of phosphorylation and neuronal activity on PKD-2 ciliary localization, we generated a PKD-2 mutant that does not form a normal channel but still localizes to cilia. The carboxy terminus of human PC-2 is important for its interaction with PC-1, channel properties, and subcellular localization (Qian *et al.*, 1997; Cai *et al.*, 1999, 2004; Chen *et al.*, 2001; Nauli *et al.*, 2003; Kottgen *et al.*, 2005). Two pathogenic C-terminal truncations of PC-2, L703X, and R742X (corresponding to W554 and K582 in *C. elegans* PKD-2) are found in some affected ADPKD families, illustrating the importance of this region (Chen *et al.*, 2001; Koulen *et al.*, 2002). PKD-2Δ541-716::GFP deletes the majority of the cytoplasmic carboxy terminus, does not rescue the *pkd-2* mutant (Figure 6b), but localizes to cilia (unpublished data and Figure 6c). These data indicate that the C-terminus of PKD-2 is essential for function but not ciliary localization. We generated PKD-2 $^{S534D}$Δ541-716::GFP, predicting that this mutant would localize to cilia, be insensitive to calcineurin down-regulation (no activity and calcium entry = no calcineurin activity), and be stable in wild-type adult cilia. Indeed, PKD-2::GFP, PKD-2Δ541-716::GFP, and PKD-2$^{S534D}$Δ541-716::GFP exhibit similar fluorescent intensity levels in cilia of adult males (Figure 6c).

To further test the model that calcineurin modulates PKD-2 ciliary localization via the S534 site, phospho-defective PKD-2$^{S534A}$::GFP subcellular localization was examined in the *tax-6(p675)* loss-of-function mutant. If PKD-2 ciliary localization is dependent on phosphorylation state and channel activity, then PKD-2$^{S534A}$ should be insensitive to calcineurin and equally stable in wild-type and *tax-6(p675)* mutant cilia. As predicted, we find that the PKD-2$^{S534A}$::GFP fluorescent intensity ratio (cilium/cell body) is similar in wild-type and *tax-6(p675)* (Figure 5f). This is in contrast to the greatly reduced ciliary localization of PKD-2::GFP in *tax-6(p675)* (Figure 5, b and c). Combined, these data suggest that calcineurin dephosphorylates the PKD-2$^{S534}$ site to modulate its ciliary localization. Additionally, these results confirm that *tax-6* is not essential for *pkd-2* expression or ciliogenesis.

## CONCLUSIONS

We show that CK2 and calcineurin modulate TRPP function and ciliary localization in vivo. LOV-1 and PKD-2 might assemble into a single channel or be components of a large complex like the *Drosophila* TRP complex or *C. elegans* mechanotransduction apparatus (Goodman and Schwarz, 2003; Montell, 2003). We propose that the PLAT domain of *C. elegans* LOV-1 or human PC-1 coordinates CK2 localization and activity to a key PKD-2/PC-2 CK2 site (Figure 6d). On stimulation, the polycystin mechanosensitive complex is activated (Nauli *et al.*, 2003) and phosphorylated by CK2 causing an increase in intracellular $Ca^{2+}$. Although it has not been demonstrated that PKD-2 forms a calcium-permeable in vivo, the mammalian polycystins conduct $Ca^{2+}$ in several cell types and *C. elegans* PKD-2 conducts calcium in black lipid membranes (Koulen *et al.*, 2005). Elevation in intracellular $Ca^{2+}$ concentration activates TAX-6/calcineurin, resulting in dephosphorylation of PKD-2/PC-2 and a return to an inactive state. Phosphorylation of PKD-2/PC-2 may serve as a mechanism for modulating channel properties, for attenuation of sensory signals, for clustering of channels, receptors, and signaling molecules, or for receptor internalization. In *C. elegans*, an imbalance between inactive and active PKD-2 states culminates in functional defects represented by a reduction in male mating behavior. CK2 and calcineurin have been individually implicated in other behaviors such as *Drosophila* circadian rhythms and mammalian learning and memory, respectively (Blau, 2003; Lee and Ahnn, 2004) as well as the regulation of ion channel activity and/or localization (Kuhara *et al.*, 2002; Bildl *et al.*, 2004; Cai *et al.*, 2004; Misonou *et al.*, 2004; Kottgen *et al.*, 2005; Mohapatra and Nau, 2005; Wu *et al.*, 2005). Our results provide the first demonstration of a coordinated and antagonistic relationship between the two.

CK2 is constitutively active in most systems. The model proposed in Figure 6d may be initiated by structural changes in LOV-1 protein or the entire polycystin complex after a putative mechanical stimulation. A conformational change may place CK2 in close proximity to PKD-2$^{S534}$, resulting in phosphorylation. Alternatively, it has been demonstrated that the regulated timing and localization of CK2 activity are important for phospho-regulation of diverse processes ranging from cell division to circadian rhythms (Allende and Allende, 1995; Lin *et al.*, 2002). CK2 activity is regulated by protein kinase C and inositol phosphates and increased several fold following neuronal-induced elevation of cytosolic calcium levels (Charriaut-Marlangue *et al.*, 1991; Blanquet, 1998, 2000; Boehning and Snyder, 2003; Solyakov *et al.*, 2004). Recently, PP2A has been shown to regulate CK2 activity to modulate the phosphorylation status of the $Ca^{2+}$-activated $K^+$ channel (Bildl *et al.*, 2004). Finally, the activity of CK2 may be controlled by the regulatory b subunit (Pinna, 2002). In the LOV-1/PKD-2 pathway, CK2 may be similarly regulated. However, we have no direct evi-

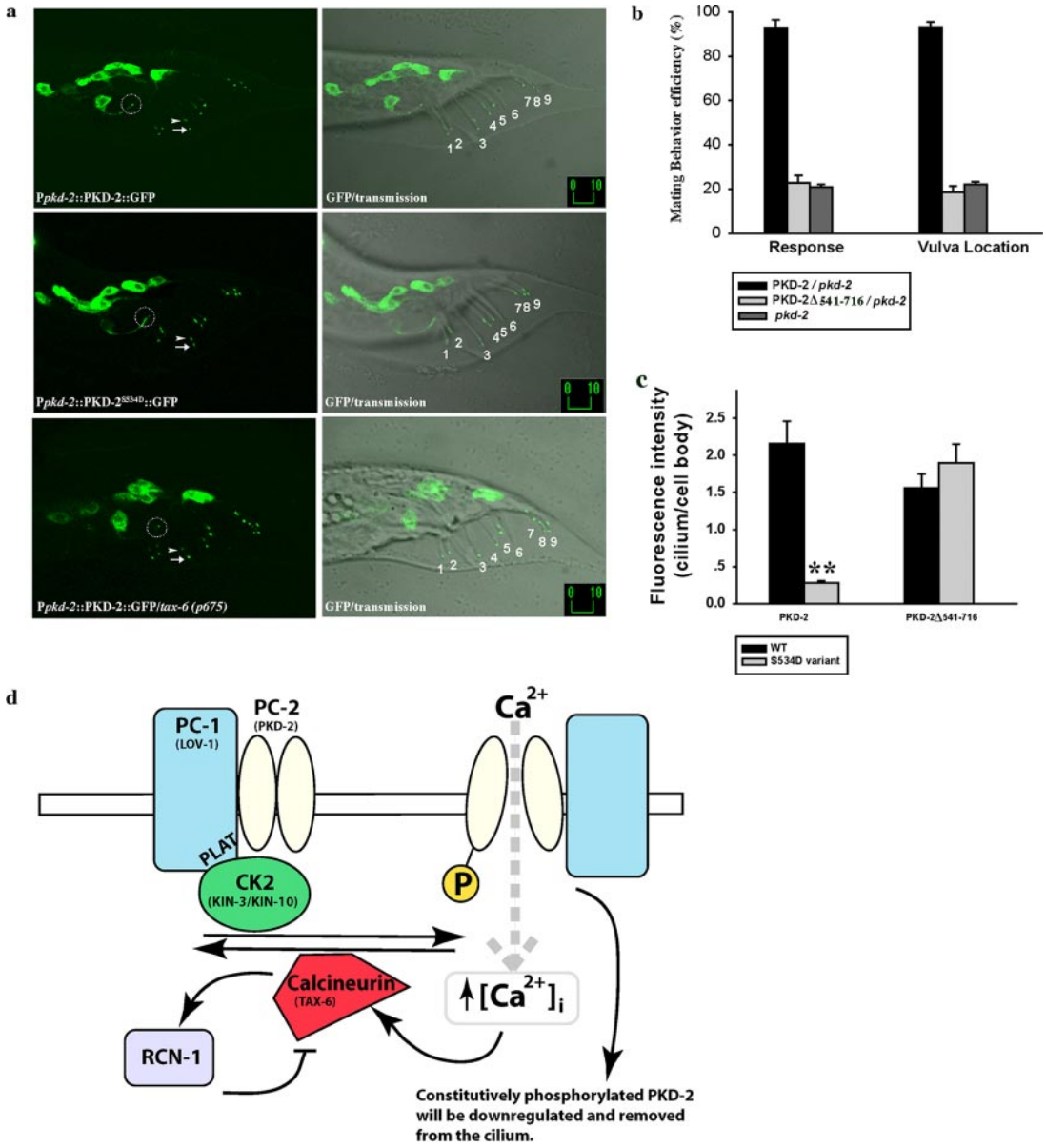


**Figure 6.** PKD-2 ciliary localization is modulated by phosphorylation and neuronal activity. (a) Confocal micrographs of PKD-2::GFP in a late L4 wild-type male tail (top), PKD-2$^{S534D}$::GFP in a late L4 wild-type male tail (middle), and PKD-2::GFP in a late L4 *tax-6(p675)* male tail (bottom). In late L4, PKD-2::GFP and PKD-2$^{S534D}$::GFP localize mainly to the ciliary tip and transition zone of sensory ray neurons. Note there is no difference in ciliary PKD-2 or PKD-2 $^{S534D}$ localization between the three transgenic animals. Arrowheads indicate the PKD-2::GFP localization around the transition zone. Arrows indicate PKD-2::GFP localization at the ciliary tip. Numbers indicate the corresponding rays. (b) In adult males, PKD-2Δ541-716::GFP fails to rescue *pkd-2* mutant defects and is a functional null. PKD-2Δ541-716::GFP is expressed and localized as wild-type PKD-2::GFP (unpublished data). (c) In adult males, PKD-2 $^{S534D}$Δ541-716::GFP ciliary localization is comparable to wild-type PKD-2 and PKD-2Δ541-716. Only active PKD-2 $^{S534D}$::GFP is down-regulated and removed from cilia. (d) Model of polycystin regulation by CK2 and calcineurin. In wild-type sensory cilia, the PLAT domain of LOV-1 docks CK2$\beta$ in close proximity to PKD-2. On stimulation, PKD-2 is phosphorylated by CK2, enhancing channel activity. Elevation in intracellular $Ca^{2+}$ concentration activates TAX-6/Calcineurin, resulting in dephosphorylation of PKD-2 and a return to an inactive state. A balance between phosphorylation and dephosphorylation is required for cellular homeostasis and the regulation of polycystin signaling. When S534 phosphorylation of PKD-2 is blocked (by CK2 RNAi, *tax-6* gain-of-function, *rcn-1* RNAi, or the PKD-2$^{S534A}$ mutation), PKD-2 signaling is impaired. When S534 phosphorylation of PKD-2 is constitutive (by *tax-6* loss-of-function or the PKD-2 $^{S534D}$ mutation), the PKD-2 channel may be hyperactivated. Dysregulated intracellular calcium elevation may lead to protein-trafficking defects, such as the down-regulation and removal of PKD-2 from the cilium, which may be mediated by ubiquitylation.

dence proving that CK2 activation occurs downstream of calcium entry through LOV-1/PKD-2 after mating.

Posttranslational modification of receptors is a common theme in the regulation of vertebrate sensory signal transduction. This study demonstrates a role for calcineurin in regulating ciliary protein localization and elucidates a novel mechanism for targeting CK2 to the TRPP complex. Interestingly, CK2 has been implicated in the regulation of mammalian PC-2 activity and trafficking to the plasma membrane (Cai *et al.*, 2004; Kottgen *et al.*, 2005) and PC-1 has been shown to activate a calcineurin/NFAT (nuclear factor of activated T-cells) signaling pathway (Puri *et al.*, 2004). Mam-

malian PC-2$^{S812}$ is constituitively phosphorylated in vivo (Cai *et al.*, 2004). This CK2 site (S812) is not conserved in *C. elegans* PKD-2. Walz and colleagues have shown that trafficking of PC-2 from the ER to the plasma membrane involves CK2 phosphorylation at S812 in an acidic cluster region and PACS proteins (Kottgen *et al.*, 2005). There are no data to suggest that S812 is critical for PC-2 ciliary localization nor is there an acidic cluster region found in *C. elegans* PKD-2. Distinct mechanisms are likely required for localizing polycystin-2 to the ER, plasma membrane, and cilium. Our studies address the latter. The PKD-2 S534 CK2 phosphorylation site is conserved between *C. elegans* and mammalian PC-2 (Harteneck *et al.*, 2000; Figure 3a). A role for the comparable *C. elegans* PKD-2 S534 site in mammalian PC-2 (S681 in mouse and T683 in human) has not been explored.

Our data suggest that PKD-2 phosphosphorylation state and TAX-6/calcineurin play pivotal roles in modulating ciliary sensory receptor localization, possibly be regulating PKD-2 recycling and turnover. Interestingly, the PKD-2 carboxy terminus interacts with an ubiquitin family member in the yeast two-hybrid system (D. R. Braun, J. Hu, and M. M. Barr, unpublished results) and human PC-1 binds and is regulated by Siah-1 (seven in absentia homolog) through the ubiquitin-proteasome pathway (Kim *et al.*, 2004). Whether or not the polycystin complex or other ciliary sensory receptors are down-regulated by ubiquitylation in vivo is an open and intriguing question.

These studies also raise the question of how natural sensory stimuli regulate polycystin subcellular distribution. Although the nature of the LOV-1/PKD-2 polycystin ligand is not known, chemical and mechanical cues appear to be required for vulva location (M. M. Barr and Paul W. Sternberg, unpublished results). The mammalian polycystin complex is mechanically gated in kidney primary cilia (Nauli *et al.*, 2003). How does male mating behavior affect PKD-2::GFP ciliary localization in worm neurons? How does urine flow modulate polycystin ciliary localization in kidney tubules? To date, we have not observed any obvious differences in PKD-2 ciliary localization before and after mating. However, PKD-2::GFP particles move along the dendrite in both anterograde (from cell body to cilia base) and retrograde (from cilia base to cell body) directions, suggesting that the ciliary PKD-2 pool may be dynamically modulated (Bae, Y. K., Qin, H., Knobel, K. M., Hu, J., Rosenbaum, J. L., and Barr, M. M., unpublished results).

The PLAT domain of polycystin-1 may serve as a docking site for interacting proteins. Previously, we described an interaction between the PLAT domain of LOV-1 and human PC-1 with the beta subunit of the F1-ATP synthase (ATP-2; Hu and Barr, 2005). In *C. elegans*, ATP-2 and other ATP synthase components localize to cilia and act in the polycystin-signaling pathway to control male sensory behaviors. Here, we show that CK2$\beta$ interacts with the PLAT domain of worm LOV-1 and human PC-1. The finding that CK2$\beta$-PLAT domain association and CK2 site in PKD-2/PC-2 are evolutionarily conserved supports the hypothesis that a dynamic phosphorylation cycle modulates polycystin function and subcellular localization. Understanding the mechanism(s) of phosphorylation and dephosphorylation of ion channels in general and specifically the polycystins may have clinical relevance in terms of treating ADPKD patients and the prevention of cyst growth and end-stage renal disease.

## ACKNOWLEDGMENTS

We thank Dr. K. Ling for help on mammalian cell expression and immunoprecipitation; Dr. A. Fire for plasmids; Dr. J. Ahnn, the *Caenorhabditis* Genetics Center, Dr. S. Mitani, and the Japanese National Bioresource Project for the Nematode for strains; T. Liu and the two anonymous reviewers for critical comments on this manuscript; and D. Braun for excellent technical assistance. This research is supported by grants from the Polycystic Kidney Disease Foundation (J.H. and K.M.K.) and National Institutes of Health (M.M.B.).

## REFERENCES

Allende, J. E., and Allende, C. C. (1995). Protein kinase CK2, an enzyme with multiple substrates and a puzzling regulation. FASEB J. *9*, 313–323.

Bandyopadhyay, J., Lee, J., Lee, J. I., Yu, J. R., Jee, C., Cho, J. H., Jung, S., Lee, M. H., Zannoni, S., Singson, A., Kim do, H., Koo, H. S., and Ahnn, J. (2002). Calcineurin, a calcium/calmodulin-dependent protein phosphatase, is involved in movement, fertility, egg laying, and growth in *Caenorhabditis elegans*. Mol. Biol. Cell *13*, 3281–3293.

Barr, M. M. (2005). *Caenorhabditis elegans* as a model to study renal development and disease: sexy cilia. J. Am. Soc. Nephrol. *16*, 305–312.

Barr, M. M., DeModena, J., Braun, D., Nguyen, C. Q., Hall, D. H., and Sternberg, P. W. (2001). The *Caenorhabditis elegans* autosomal dominant polycystic kidney disease gene homologs *lov-1* and *pkd-2* act in the same pathway. Curr. Biol. *11*, 1341–1346.

Barr, M. M., and Sternberg, P. W. (1999). A polycystic kidney-disease gene homologue required for male mating behaviour in *C. elegans*. Nature *401*, 386–389.

Bateman, A., and Sandford, R. (1999). The PLAT domain: a new piece in the PKD1 puzzle. Curr. Biol. *9*, R588–590.

Bildl, W., Strassmaier, T., Thurm, H., Andersen, J., Eble, S., Oliver, D., Knipper, M., Mann, M., Schulte, U., Adelman, J. P., and Fakler, B. (2004). Protein kinase CK2 is coassembled with small conductance Ca(2+)-activated K+ channels and regulates channel gating. Neuron *43*, 847–858.

Blanquet, P. R. (1998). Neurotrophin-induced activation of casein kinase 2 in rat hippocampal slices. Neuroscience *86*, 739–749.

Blanquet, P. R. (2000). Casein kinase 2 as a potentially important enzyme in the nervous system. Prog Neurobiol *60*, 211–246.

Blau, J. (2003). A new role for an old kinase: CK2 and the circadian clock. Nat. Neurosci. *6*, 208–210.

Boehning, D., and Snyder, S. H. (2003). Novel neural modulators. Annu. Rev. Neurosci. *26*, 105–131.

Brenner, S. (1974). The genetics of *Caenorhabditis elegans*. Genetics *77*, 71–94.

Cai, Y. *et al.* (2004). Calcium dependence of polycystin-2 channel activity is modulated by phosphorylation at Ser812. J. Biol. Chem. *279*, 19987–19995.

Cai, Y., Maeda, Y., Cedzich, A., Torres, V. E., Wu, G., Hayashi, T., Mochizuki, T., Park, J. H., Witzgall, R., and Somlo, S. (1999). Identification and characterization of polycystin-2, the PKD2 gene product. J. Biol. Chem. *274*, 28557–28565.

Chantalat, L., Leroy, D., Filhol, O., Nueda, A., Benitez, M. J., Chambaz, E. M., Cochet, C., and Dideberg, O. (1999). Crystal structure of the human protein kinase CK2 regulatory subunit reveals its zinc finger-mediated dimerization. EMBO J. *18*, 2930–2940.

Charriaut-Marlangue, C., Otani, S., Creuzet, C., Ben-Ari, Y., and Loeb, J. (1991). Rapid activation of hippocampal casein kinase II during long-term potentiation. Proc. Natl. Acad. Sci. USA *88*, 10232–10236.

Chen, X. Z., Segal, Y., Basora, N., Guo, L., Peng, J. B., Babakhanlou, H., Vassilev, P. M., Brown, E. M., Hediger, M. A., and Zhou, J. (2001). Transport function of the naturally occurring pathogenic polycystin-2 mutant, R742X. Biochem. Biophys. Res. Commun. *282*, 1251–1256.

Chen, X. Z., Vassilev, P. M., Basora, N., Peng, J. B., Nomura, H., Segal, Y., Brown, E. M., Reeders, S. T., Hediger, M. A., and Zhou, J. (1999). Polycystin-L is a calcium-regulated cation channel permeable to calcium ions. Nature *401*, 383–386.

Clapham, D. E. (2003). TRP channels as cellular sensors. Nature *426*, 517–524.

Collet, J., Spike, C. A., Lundquist, E. A., Shaw, J. E., and Herman, R. K. (1998). Analysis of osm-6, a gene that affects sensory cilium structure and sensory neuron function in *Caenorhabditis elegans*. Genetics *148*, 187–200.

Delmas, P. (2004). Polycystins: from mechanosensation to gene regulation. Cell *118*, 145–148.

Faust, M., and Montenarh, M. (2000). Subcellular localization of protein kinase CK2. A key to its function? Cell Tissue Res. *301*, 329–340.

Fraser, A. G., Kamath, R. S., Zipperlen, P., Martinez-Campos, M., Sohrmann, M., and Ahringer, J. (2000). Functional genomic analysis of *C. elegans* chromosome I by systematic RNA interference. Nature *408*, 325–330.

Gao, Z., Joseph, E., Ruden, D. M., and Lu, X. (2004). *Drosophila* Pkd2 is haploid-insufficient for mediating optimal smooth muscle contractility. J. Biol. Chem. *279*, 14225–14231.

Gao, Z., Ruden, D. M., and Lu, X. (2003). PKD2 cation channel is required for directional sperm movement and male fertility. Curr. Biol. *13*, 2175–2178.

Goodman, M. B., and Schwarz, E. M. (2003). Transducing touch in *Caenorhabditis elegans.* Annu. Rev. Physiol. *65*, 429–452.

Gottschalk, A., Almedom, R. B., Schedletzky, T., Anderson, S. D., Yates, J. R., and Schafer, W. R. (2005). Identification and characterization of novel nicotinic receptor-associated proteins in *Caenorhabditis elegans*. EMBO J. *24*, 2566–2578.

Granato, M., Schnabel, H., and Schnabel, R. (1994). pha-1, a selectable marker for gene transfer in *C. elegans.* Nucleic Acids Res. *22*, 1762–1763.

Greif, D. M., Sacks, D. B., and Michel, T. (2004). Calmodulin phosphorylation and modulation of endothelial nitric oxide synthase catalysis. Proc. Natl. Acad. Sci. USA *101*, 1165–1170.

Hanaoka, K., Qian, F., Boletta, A., Bhunia, A. K., Piontek, K., Tsiokas, L., Sukhatme, V. P., Guggino, W. B., and Germino, G. G. (2000). Co-assembly of polycystin-1 and -2 produces unique cation-permeable currents. Nature *408*, 990–994.

Harteneck, C., Plant, T. D., and Schultz, G. (2000). From worm to man: three subfamilies of TRP channels. Trends Neurosci. *23*, 159–166.

Hodgkin, J. (1983). Male phenotypes and mating efficiency in *Caenorhabditis elegans*. Genetics *103*, 43–64.

Hu, J., and Barr, M. M. (2005). ATP-2 Interacts with the PLAT domain of LOV-1 and is involved in *Caenorhabditis elegans* polycystin signaling. Mol. Biol. Cell *16*, 458–469.

Hughes, J., Ward, C. J., Peral, B., Aspinwall, R., Clark, K., San Millan, J. L., Gamble, V., and Harris, P. C. (1995). The polycystic kidney disease 1 (PKD1) gene encodes a novel protein with multiple cell recognition domains. Nat. Genet. *10*, 151–160.

Igarashi, P., and Somlo, S. (2002). Genetics and pathogenesis of polycystic kidney disease. J. Am. Soc. Nephrol. *13*, 2384–2398.

Kim, H., Jeong, W., Ahn, K., Ahn, C., and Kang, S. (2004). Siah-1 interacts with the intracellular region of polycystin-1 and affects its stability via the ubiquitin-proteasome pathway. J. Am. Soc. Nephrol. *15*, 2042–2049.

Kottgen, M. *et al.* (2005). Trafficking of TRPP2 by PACS proteins represents a novel mechanism of ion channel regulation. EMBO J. *24*, 705–716.

Koulen, P., Cai, Y., Geng, L., Maeda, Y., Nishimura, S., Witzgall, R., Ehrlich, B. E., and Somlo, S. (2002). Polycystin-2 is an intracellular calcium release channel. Nat. Cell Biol. *4*, 191–197.

Koulen, P., Duncan, R. S., Liu, J., Cohen, N. E., Yannazzo, J. A., McClung, N., Lockhart, C. L., Branden, M., and Buechner, M. (2005). Polycystin-2 accelerates $Ca^{2+}$ release from intracellular stores in *Caenorhabditis elegans.* Cell Calcium *37*, 593–601.

Kuhara, A., Inada, H., Katsura, I., and Mori, I. (2002). Negative regulation and gain control of sensory neurons by the *C. elegans* calcineurin TAX-6. Neuron *33*, 751–763.

Kunitomo, H., Uesugi, H., Kohara, Y., and Iino, Y. (2005). Identification of ciliated sensory neuron-expressed genes in *Caenorhabditis elegans* using targeted pull-down of poly(A) tails. Genome Biol. *6*, R17.

Lee, J., Jee, C., Song, H. O., Bandyopadhyay, J., Lee, J. I., Yu, J. R., Lee, J., Park, B. J., and Ahnn, J. (2004). Opposing functions of calcineurin and CaMKII regulate G-protein signaling in egg-laying behavior of *C. elegans.* J. Mol. Biol. *344*, 585–595.

Lee, J., Song, H. O., Jee, C., Vanoaica, L., and Ahnn, J. (2005). Calcineurin regulates enteric muscle contraction through EXP-1, excitatory GABA-gated channel, in *C. elegans.* J. Mol. Biol. *16*, 313–318.

Lee, J. I., and Ahnn, J. (2004). Calcineurin in animal behavior. Mol. Cell *17*, 390–396.

Lee, J. I., Dhakal, B. K., Lee, J., Bandyopadhyay, J., Jeong, S. Y., Eom, S. H., Kim do, H., and Ahnn, J. (2003). The *Caenorhabditis elegans* homologue of Down syndrome critical region 1, RCN-1, inhibits multiple functions of the phosphatase calcineurin. J. Mol. Biol. *328*, 147–156.

Lin, J. M., Kilman, V. L., Keegan, K., Paddock, B., Emery-Le, M., Rosbash, M., and Allada, R. (2002). A role for casein kinase 2alpha in the *Drosophila* circadian clock. Nature *420*, 816–820.

Lipton, J., Kleemann, G., Ghosh, R., Lints, R., and Emmons, S. W. (2004). Mate searching in *Caenorhabditis elegans*: a genetic model for sex drive in a simple invertebrate. J. Neurosci. *24*, 7427–7434.

Litchfield, D. W. (2003). Protein kinase CK2, structure, regulation and role in cellular decisions of life and death. Biochem. J. *369*, 1–15.

Liu, K. S., and Sternberg, P. W. (1995). Sensory regulation of male mating behavior in *Caenorhabditis elegans.* Neuron *14*, 79–89.

Meggio, F., and Pinna, L.A. (2003). One-thousand-and-one substrates of protein kinase CK2? FASEB J. *17*, 349–368.

Mello, C., and Fire, A. (1995). DNA transformation. Methods Cell Biol. *48*, 451–482.

Misonou, H., Mohapatra, D. P., Park, E. W., Leung, V., Zhen, D., Misonou, K., Anderson, A. E., and Trimmer, J. S. (2004). Regulation of ion channel localization and phosphorylation by neuronal activity. Nat. Neurosci. *7*, 711–718.

Mochizuki, T. *et al.* (1996). PKD2, a gene for polycystic kidney disease that encodes an integral membrane protein. Science *272*, 1339–1342.

Mohapatra, D. P., and Nau, C. (2005). Regulation of Ca2+-dependent desensitization in the vanilloid receptor TRPV1 by calcineurin and cAMP-dependent protein kinase. J. Biol. Chem. *280*, 13424–13432.

Montell, C. (2003). The venerable inveterate invertebrate TRP channels. Cell Calcium *33*, 409–417.

Nauli, S. M. *et al.* (2003). Polycystins 1 and 2 mediate mechanosensation in the primary cilium of kidney cells. Nat. Genet. *33*, 129–137.

Niefind, K., Guerra, B., Ermakowa, I., and Issinger, O. G. (2001). Crystal structure of human protein kinase CK2, insights into basic properties of the CK2 holoenzyme. EMBO J. *20*, 5320–5331.

Orozco, J. T., Wedaman, K. P., Signor, D., Brown, H., Rose, L., and Scholey, J. M. (1999). Movement of motor and cargo along cilia. Nature *398*, 674

Peden, E. M., and Barr, M. M. (2005). The KLP-6 kinesin is required for male mating behaviors and polycystin localization in *Caenorhabditis elegans.* Curr. Biol. *15*, 394–404.

Pinna, L. A. (2002). Protein kinase CK2, a challenge to canons. J. Cell Sci. *115*, 3873–3878.

Puri, S., Magenheimer, B. S., Maser, R. L., Ryan, E. M., Zien, C. A., Walker, D. D., Wallace, D. P., Hempson, S. J., and Calvet, J. P. (2004). Polycystin-1 activates the calcineurin/NFAT (nuclear factor of activated T-cells) signaling pathway. J. Biol. Chem. *279*, 55455–55464.

Qian, F., Germino, F. J., Cai, Y., Zhang, X., Somlo, S., and Germino, G. G. (1997). PKD1 interacts with PKD2 through a probable coiled-coil domain. Nat. Genet. *16*, 179–183.

Rosenbaum, J. L., and Witman, G. B. (2002). Intraflagellar transport. Nat. Rev. Mol. Cell Biol. *3*, 813–825.

Simmer, F., Tijsterman, M., Parrish, S., Koushika, S. P., Nonet, M. L., Fire, A., Ahringer, J., and Plasterk, R. H. (2002). Loss of the putative RNA-directed RNA polymerase RRF-3 makes *C. elegans* hypersensitive to RNAi. Curr. Biol. *12*, 1317–1319.

Simon, J. M., and Sternberg, P. W. (2002). Evidence of a mate-finding cue in the hermaphrodite nematode *Caenorhabditis elegans.* Proc. Natl. Acad. Sci. USA *99*, 1598–1603.

Solyakov, L., Cain, K., Tracey, B. M., Jukes, R., Riley, A. M., Potter, B. V., and Tobin, A. B. (2004). Regulation of casein kinase-2 (CK2) activity by inositol phosphates. J. Biol. Chem. *279*, 43403–43410.

Sulston, J. E., Albertson, D. G., and Thomson, J. N. (1980). The *Caenorhabditis elegans* male: postembryonic development of nongonadal structures. Dev. Biol. *78*, 542–576.

Tavernarakis, N., Wang, S. L., Dorovkov, M., Ryazanov, A., and Driscoll, M. (2000). Heritable and inducible genetic interference by double-stranded RNA encoded by transgenes. Nat. Genet. *24*, 180–183.

Wang, J., and Barr, M. M. (2005). RNA Interference in *Caenorhabditis elegans.* Methods Enzymol. *392*, 36–55.

Watnick, T. J., Jin, Y., Matunis, E., Kernan, M. J., and Montell, C. (2003). A flagellar polycystin-2 homolog required for male fertility in *Drosophila.* Curr. Biol. *13*, 2179–2184.

Wu, Z. Z., Chen, S. R., and Pan, H. L. (2005). TRPV1 activation downregulates voltage-gated calcium channels through calcium-dependant calcineurin in sensory neurons. J. Biol. Chem. *280*, 18142–18151.